NATIONAL ADVISORY COMMITTEE FOR AERONAUTICS

TECHNICAL NOTE 4359

A REVIEW OF THE THERMODYNAMIC, TRANSPORT, AND CHEMICAL REACTION RATE PROPERTIES OF HIGH-TEMPERATURE AIR

By C. Frederick Hansen and Steve P. Heims

Ames Aeronautical Laboratory
Moffett Field, Calif.

Washington
July 1958

NATIONAL ADVISORY COMMITTEE FOR AERONAUTICS

TECHNICAL NOTE 4359

A REVIEW OF THE THERMODYNAMIC, TRANSPORT, AND CHEMICAL REACTION RATE PROPERTIES OF HIGH-TEMPERATURE AIR

By C. Frederick Hansen and Steve P. Heims

INTRODUCTION

It is axiomatic that the science of aerodynamics must be based on a good understanding of the atmospheric medium through which vehicles are to fly. It is well known that vehicles traveling at high speed excite the air to high temperatures, with the result that air properties deviate considerably from those of a simple gas which obeys the ideal gas law and which has a constant specific heat. For example, figure 1 shows the major chemical reactions which are produced in the stagnation regions of vehicles traveling at high velocity through the atmosphere. At about 3,000 feet per second the vibrational energy of air molecules begins to become important. Oxygen dissociation begins at 6,000 to 8,000 feet per second, nitrogen dissociation occurs at velocities in excess of 15,000 feet per second, and, finally, ionization of atoms becomes of major importance near escape velocity. The dissociation and ionization reactions are pressure dependent because each particle yields two product particles, and such reactions are inhibited by high pressure. Therefore, higher temperature and, consequently, higher velocity are required to produce the reactions at sea level than at high altitudes where much lower pressures occur. Vibrational energy is excited wherever molecules exist at high temperature, and so the domain in which vibrational excitation is important continues throughout the regions of the dissociation reactions as well. It can be intuitively appreciated that these reactions will affect many of the properties of air. Some of these properties which will not be considered herein may have important aerodynamic effects; for example, the electrical conductivity is a fundamental parameter in magnetohydrodynamics. The present discussion, however, is limited to the thermodynamic and transport properties and to the reaction rates for the chemical processes which occur in air. The thermodynamic properties include the energy, enthalpy, entropy, specific heats, and the speed of sound for air; the transport properties to be considered are the viscosity and thermal conductivity; and the most important reaction rates are those for the chemical processes indicated in figure 1. In the absence of magnetohydrodynamic effects, these parameters are the fundamental ones that determine the characteristics of air flow.

THERMODYNAMIC PROPERTIES OF AIR

The equilibrium thermodynamic properties of air can be calculated to very high temperatures with considerable confidence, since the molecular and atomic energy levels on which these calculations are based are known very precisely from spectroscopic data (refs. 1 and 2). Gilmore (ref. 3) and later Hilsenrath and Beckett (ref. 4) have prepared accurate tables of thermodynamic functions for air. Before discussing the features of these functions in detail, it will be helpful to review briefly the expressions for energy of atoms and diatomic molecules. Mechanical analogies will be used freely in this discussion. These should not be taken as exact descriptions of the atomic and molecular systems, of course.

Figure 2(a) shows a ball and spring model for the diatomic molecule which is vibrating and rotating at the same time that it is in translational motion. The energy of this molecule is a function of its velocity u, the rotational quantum number J, and the vibrational quantum number n, as shown in the following equation:

$$e(u,J,n) = \frac{mu^2}{2} + J(J + 1)\frac{h^2}{2I} + nh\nu$$

where

m mass of molecule

h Planck's constant

I moment of inertia

ν characteristic frequency of molecular bond (the spring)

At high temperatures, the electrons may also be excited to quantum states above the ground state, but this contribution to total energy is generally rather small and, therefore, is omitted herein for purposes of simplification. If one averages this molecular energy over a large number of molecules in a sample of gas at a temperature T, the average energy per mol is given by the following equation:

$$E = \frac{3}{2}RT + RT + RT\left(\frac{h\nu}{kT}\right)\left(e^{\frac{h\nu}{kT}} - 1\right)^{-1}$$

The translational motion contributes $\frac{3}{2}RT$, and the rotation contributes an average energy which asymptotically approaches RT. The characteristic temperature T_r at which rotational energy is half excited is of

the order of 5° K, so that, for most practical purposes, air molecules in the gas phase are always fully excited in rotation. On the other hand, the molecular bond is so stiff that at normal temperatures the molecules are essentially rigid rotators. However, as temperature increases, the molecular collisions eventually become energetic enough to set the bond into vibration. The vibrational energy is roughly half excited at the characteristic temperature $h\nu/k$. This temperature is rather high, being the order of $3{,}000^{\circ}$ K.

The specific heat at constant density is the derivative of the average energy with respect to temperature. This specific heat for diatomic molecules is shown graphically in figure 2(a). It is already $5R/2$ at very low temperatures and maintains a relatively constant value throughout the range of temperatures encountered at subsonic and low supersonic flight speeds. As vibrational energy becomes important at higher temperatures, the specific heat approaches $7R/2$.

At still higher temperatures, the molecular impacts become so intense that the bond is often stretched to the breaking point. Figure 2(b) illustrates a collision between two molecules which has just resulted in the dissociation of one of the molecules into two atoms. Again, if electronic energy is neglected, the energy of each atom is its kinetic energy plus one-half the energy stored in the broken bond $e_o/2$, as shown in the following equation:

$$e(u) = \left(\frac{m}{2}\right)\frac{u^2}{2} + \frac{e_o}{2}$$

The average energy for a mol of atoms at a temperature T is

$$E = \frac{3}{2}RT + \frac{D}{2}$$

As before, the kinetic energy contributes $\frac{3}{2}RT$. The constant e_o is independent of temperature or velocity and contributes to the average energy the heat needed to dissociate 1 mol of the molecules D. The ratio D/R is of the order of $50{,}000^{\circ}$ K for oxygen and $100{,}000^{\circ}$ K for nitrogen, so that the dissociation energy term is much larger than the average kinetic energy at the temperatures of interest in this study (up to about $15{,}000^{\circ}$ K). The specific heat dE/dT of the atoms, from figure 2(b), is about $\frac{3}{2}R$. The large constant term $D/2$ does not contribute to the derivative, of course.

Figure 3 shows the energy and specific heats for molecule-atom mixtures in equilibrium. In the following equations:

Energy:

$$E = (1 - x)E_m + xE_a$$

Specific heat:

$$\frac{\partial E}{\partial T} = (1 - x)\frac{dE_m}{dT} + x\frac{dE_a}{dT} - E_m\frac{\partial x}{\partial T} + (E_a)\frac{\partial x}{\partial T}$$

E_m and E_a are, respectively, the average energy per mol of molecules and of atoms, which has just been considered. The mol fraction of atoms x is a function of the chemical equilibrium constant K and pressure p, which can be calculated precisely (ref. 3), and the mol fraction of molecules is $1 - x$. In the equation for specific heat, the first two terms on the right-hand side are the sum of the specific heats for the components of the mixture, whereas the last two terms give the contribution due to the change in mol fractions. The derivative $\partial x/\partial T$, which can be expressed as a function of x and the logarithmic derivative of the equilibrium constant, possesses a rather sharp maximum. The value of $\partial x/\partial T$ is small, but the value of E_a is so large, because of the dissociation energy, that, where the mol fraction derivative is a maximum, the last term in the specific-heat equation is overwhelmingly predominant.

The graph in figure 3 shows the specific heat for air as a function of temperature at a pressure of 0.01 atmosphere and illustrates the striking effect of the chemical reactions. Near 3,000° K the specific heat has a pronounced maximum due to dissociation of oxygen, and again near 5,000° K the nitrogen dissociation is responsible for another peak. The last peak, near 10,000° K, is due to the reactions for single ionization of nitrogen and oxygen atoms. These two reactions occur together in the same range of temperature and a similar set of relations is obtained as for the dissociation reactions, except that the ionization energy I is larger than the dissociation energy (I/R is of the order of 150,000° K). The effect of pressure is that the maximums become larger and more peaked and shift to lower temperatures as pressure decreases.

It is convenient to relate the chemical reactions in air to the compressibility factor Z. This factor is the number of moles of gas which arise from a mol of air originally at normal conditions or, alternatively, it is the ratio of the molecular weight of normal air to the mean molecular weight of the equilibrium gas. It represents the

correction factor to the ideal gas equation of state. Figure 4 shows the compressibility factor for air as a function of temperature for pressures of 1.0, 0.01, and 0.0001 atmosphere.

The important reactions in air are also indicated in figure 4. These are: (1) the dissociation of oxygen

$$O_2 \leftrightarrows 2O$$

(2) the dissociation of nitrogen

$$N_2 \leftrightarrows 2N$$

and (3) the reactions for single ionization of nitrogen and oxygen atoms

$$N \leftrightarrows N^+ + e^-$$

$$O \leftrightarrows O^+ + e^-$$

The ionization reactions occur at very nearly the same temperature and with nearly the same energy changes so that they may be classed together as a single reaction, for purposes of approximation.

The foregoing reactions are the ones which largely determine the equilibrium concentration of the major components of air, and these components, in turn, establish the thermodynamic properties. At high pressures, nitric oxide NO becomes a sizable minor component of air but the thermodynamic properties of NO are about the average of those for N_2 and O_2, and, since the nitric oxide formation does not change the balance between molecules and atoms, it does not greatly influence the thermodynamic functions of air.

The compressibility is not influenced by vibrational excitation and, therefore, is equal to 1.0 until oxygen dissociation begins. Since air contains about 20 percent oxygen, the compressibility approaches 1.2 when oxygen dissociation is complete. It increases further to a value of 2.0 when nitrogen dissociation finishes the conversion of molecules into atoms. Single ionization of the atoms doubles the number of gas particles again, so that the compressibility approaches 4.0 when these reactions are complete.

The effects of the chemical reactions are most intense where the slope of the compressibility is a maximum. The most interesting feature of these functions is that the slope of Z is nearly zero at the transition from one major reaction to another (fig. 4). This shows that one reaction is essentially complete before the next reaction starts, and in reference 5, for example, complete independence between the reactions is

assumed in order to derive analytic solutions for the properties of high-temperature air. It is found that these analytic solutions are generally within 2 percent of the precise answers obtained by iteration (ref. 4). The most time-consuming portion of such calculations is finding the compressibility factor (or its equivalent, the component mol fractions). If less accuracy is sufficient, of the order of 10 percent, the compressibility function can be fitted empirically with hyperbolic tangents. The approximate formulas for compressibility, energy, enthalpy, and the specific heats are as follows:

$$Z \approx 2.5 + 0.1 \tanh\left(\frac{\theta}{500} - 7\right) + 0.4 \tanh\left(\frac{\theta}{1000} - 7\right) + \tanh\left(\frac{\theta}{2500} - 5.8\right) \quad (1)$$

where the reduced temperature is

$$\theta = T\left(1 - \frac{1}{8} \log \frac{p}{p_o}\right) \quad (2)$$

the reference pressure p_o is 1 atmosphere, and log signifies the logarithm to the base 10. The dimensionless energy is

For case I, oxygen dissociation only ($1.0 < Z < 1.2$):

$$\frac{ZE}{RT} \approx (2 - Z)\left[\frac{5}{2} + \frac{3000}{T}\left(\exp \frac{3000}{T} - 1\right)^{-1}\right] + (Z - 1)\left(3 + \frac{59000}{T}\right) \quad (3a)$$

For case II, nitrogen dissociation only ($1.2 < Z < 2.0$):

$$\frac{ZE}{RT} \approx (2 - Z)\left[\frac{5}{2} + \frac{3000}{T}\left(\exp \frac{3000}{T} - 1\right)^{-1}\right] + 0.2\left(3 + \frac{59000}{T}\right) + (Z - 1.2)\left(3 + \frac{113000}{T}\right) \quad (3b)$$

For case III, ionization reactions only, up to about 10 percent ionization ($2.0 < Z < 2.2$):

$$\frac{ZE}{RT} \approx (4 - Z)\left(\frac{3}{2} + \frac{51000}{T}\right) + (Z - 2)\left(3 + \frac{220000}{T}\right) \quad (3c)$$

The enthalpy H is easily found from the relation

$$\frac{ZH}{RT} = \frac{ZE}{RT} + Z \quad (4)$$

For cases I and II, the entropy S is approximately given by

$$Z\left(\frac{S}{R} + \log_e \frac{p}{p_o}\right) \approx (2 - Z)\left\{\frac{7}{2}(\log_e T + 1) - \log_e\left[1 - \exp\left(-\frac{3000}{T}\right)\right] + \frac{3000}{T}\left(\exp\frac{3000}{T} - 1\right)^{-1} - \log_e \frac{2 - Z}{Z}\right\} + 2(Z - 1)\left[\frac{5}{2}(\log_e T + 1) + 2.3 - \log_e \frac{2(Z - 1)}{Z}\right] \quad (5a)$$

and for case III,

$$Z\left(\frac{S}{R} + \log_e \frac{p}{p_o}\right) \approx \frac{5Z}{2}(\log_e T + 1) + 4.6 - (Z - 2)\left(2 \log_e \frac{Z - 2}{Z} + 14.2\right) - (4 - Z)\log_e \frac{4 - Z}{Z} \quad (5b)$$

In view of the order of the approximation, an average vibrational frequency has been assumed for both oxygen and nitrogen and in the energy functions the particles are treated as though all are in the ground state of electronic excitation. Note that the displacement of the compressibility function varies as the logarithm of pressure and that the thermodynamic properties are all given as functions of compressibility and temperature. The electronic excitation has been accounted for in the entropy functions by adding constant values equal to the average of the logarithm of the electronic partition function over the temperature range of interest.

For the specific heat, the derivative of compressibility with temperature is required. It is given by

$$\left(\frac{\partial Z}{\partial T}\right)_p \approx 0.0002\left(1 - \frac{1}{8}\log \frac{p}{p_o}\right)\left[\operatorname{sech}^2\left(\frac{\theta}{500} - 7\right) + 2 \operatorname{sech}^2\left(\frac{\theta}{1000} - 7\right) + 2 \operatorname{sech}^2\left(\frac{\theta}{2500} - 5.8\right)\right] \quad (6)$$

If the correction for taking the partial derivative at constant pressure is disregarded, the specific heat at constant density becomes

For case I:

$$\frac{Zc_v}{R} \approx (2 - Z)\left[\frac{5}{2} + \left(\frac{1500/T}{\sinh \frac{1500}{T}}\right)^2\right] + 3(Z - 1) + \left(\frac{T}{2} + 59{,}000\right)\frac{\partial Z}{\partial T} \qquad (7a)$$

For case II:

$$\frac{Zc_v}{R} \approx (2 - Z)\left[\frac{5}{2} + \left(\frac{1500/T}{\sinh \frac{1500}{T}}\right)^2\right] + 3(Z - 1) + \left(\frac{T}{2} + 113{,}000\right)\frac{\partial Z}{\partial T} \qquad (7b)$$

For case III:

$$\frac{Zc_v}{R} \approx \frac{3Z}{2} + \left(\frac{3T}{2} + 167{,}000\right)\frac{\partial Z}{\partial T} \qquad (7c)$$

The specific heat at constant pressure is

$$\frac{Zc_p}{R} \approx \frac{Zc_v}{R} + Z + T\frac{\partial Z}{\partial T} \qquad (8)$$

and to the order of these approximations the speed of sound is given by

$$\frac{a^2\rho}{p} \approx \gamma = \frac{\left(\frac{Zc_p}{R}\right)}{\left(\frac{Zc_v}{R}\right)} \qquad (9)$$

The dimensionless energy is shown in figure 5 as a function of temperature for pressures of 0.0001, 0.01, and 1.0 atmosphere. The results given by the approximate formulas compare favorably with more precise calculations (refs. 4 and 5). The greatest errors occur in the region of the ionization reactions, where a simple empirical form for the compressibility function does not seem entirely adequate. Similarly, the dimensionless entropy is shown in figure 6, and again the approximate formulas compare favorably with the precise calculations until ionization temperatures are reached.

As expected, the accuracy of the approximate formulas for the specific heats is not as good as for energy, since derivatives of compressibility are involved. Still, the ratio of the specific heats is not greatly different from more precise calculations of the speed-of-sound parameter $a^2\rho/p$, as shown in figure 7. The largest deviations occur at the transitions between one reaction and the next, where the speed-of-sound parameter is a maximum.

The foregoing thermodynamic properties of air enable one to solve a number of important aerodynamic problems. Where it is desired to use analytic expressions in a computing program, the results of reference 5 may be used, or if computer storage is a problem, the analytic expressions given by equations (1) through (9) represent a compromise involving some sacrifice in accuracy. However, for many problems it is still convenient to use graphical methods of solution. The particular graphical functions which are the most convenient to use depend on the problem to be solved. For example, it is expedient to use temperature as the independent variable, as in figures 4 through 7, for processes in which temperature is constant. This must be done in the initial calculations anyway, since the partition functions are functions of temperature only. On the other hand, a Mollier type diagram in which enthalpy is plotted as a function of entropy is useful for solutions of isentropic flow processes. A very complete Mollier diagram is presented by Feldman (ref. 6). For solutions of nonisentropic flow processes such as occur in shock waves, it has been found convenient to use a graph of the dimensionless parameter $(p/h\rho)$ as a function of dimensionless enthalpy (h/h_o), where h_o is the enthalpy at standard conditions.

The properties of air which have been heated by shock waves are particularly important at the present time, because the shock tube is being used extensively as an instrument for aerodynamic testing. Romig (ref. 7) has outlined a method of solving for temperature, density, and pressure following a normal shock wave, and Feldman (ref. 6) presents a rather complete set of such solutions including the effects of oblique shocks and of shock reflections. Hochstim (ref. 8) has worked out a number of solutions for a variety of initial conditions. Perhaps one of the more usable forms in which such solutions can be presented is to graph, as a function of shock-wave Mach number, M_s, the ratio of the real gas property to the value of the same property which would occur for an ideal gas having a constant γ of 1.4. The shock-wave Mach number is defined as the speed of the shock wave divided by the speed of sound in the undisturbed air. Figures 8(a), 8(b), and 8(c) show, respectively, graphs for the pressure, density, and temperature which occur following a normal shock wave traveling through air initially at 293° K. Subscript 1 refers to the initial conditions and subscript 2 to the conditions following the normal shock wave. The superscript * denotes the ideal gas condition. The solutions are shown for initial pressures of 1, 0.1, 0.01, 0.001, and 0.0001 atmosphere. Subscript 3 will refer to the conditions following the normal reflection of the shock wave from the closed end of the shock tube, and the ratio of the real to ideal values for pressure, density, and temperature after the reflection are shown, respectively, in figures 9(a), 9(b), and 9(c). Figure 10 shows the ratio of the speed of the reflected shock wave, U_r, to the speed of a shock reflected in the ideal gas, U_r^*. The shock-wave Mach number is used as the independent variable in figures 8, 9, and 10 because the velocity is the easiest property of the shock to measure precisely. Also, the Mach number is used, rather than the velocity, because in this form it is convenient to use the solutions over a small

range of initial temperatures. While it is somewhat inconvenient to have the properties referenced to their ideal gas values, rather than plotted directly, this is more than compensated for by the fact that the gas properties can be picked off the graphs quite accurately. Note that the displacements of the curves are about proportional to the logarithm of the initial pressure, p_1, so it is possible to interpolate between the curves with reasonable accuracy also.

Obviously, not all aerodynamic problems can be solved with only the thermodynamic properties of air. Therefore we shall turn attention now to the equally important transport properties.

TRANSPORT PROPERTIES OF AIR

The transport properties of gases can all be related to the effective size of gas particles during collisions (refs. 9 and 10). The smaller the size, the larger is the mean free path between collisions; then the transport occurs between regions of the gas having greater differences in momentum and energy. Consequently, the coefficients of viscosity and thermal conductivity vary inversely with the size of the gas particles. Figure 11 shows qualitatively the form of the potential functions between the particles from which the collision diameters are determined. Consider first the potential between inert molecules. At long range, the potential has a very shallow minimum which at normal or higher temperature is very small compared with the kinetic energy of the colliding molecules. This is the portion of the potential associated with the weak Van der Waals forces of attraction. At shorter range, the potential rapidly approaches very large positive values and the interparticle forces are strongly repulsive. The path of one molecule with respect to another during collision is shown for two typical cases by the black balls which roll into the potential well, penetrate the positive column, and are deflected back into potential-free space. The depth of the penetration increases with increasing kinetic energy of the relative motion between molecules.

The effective collision diameter σ is roughly the diameter of the molecular volume which is not penetrated by the collisions and, on the average, it is approximately the diameter where the molecular potential equals $+kT$. The collision cross section is by definition $\pi\sigma^2$. From the shape of the potential, it can be seen that the collision diameter depends on the energy of the collisions and is, therefore, a function of temperature. At high temperatures, however, the extremely steep portion of the potential is penetrated and the collision cross section is relatively constant, independent of temperature. Then the molecules behave essentially as hard elastic spheres, for which the coefficient of viscosity varies as the one-half power of the temperature. The Sutherland correction to the coefficient of viscosity accounts reasonably well for the effective increase in collision diameter at low temperatures.

Where more precise estimates are required, the methods developed by Hirschfelder and others (ref. 9) are very useful for calculating the transport properties of inert gases.

The transport properties of air at high temperatures are in doubt mainly because of uncertainty about the cross sections for atom-atom and atom-molecule collisions. Two atoms, for example, may approach one another along any one of a number of different potentials depending upon how the electron spin vectors add up. This multiplicity of potentials is indicated by the dashed lines on the atom-atom potential diagram of figure 11. The only one of these potentials which is known quantitatively at present is the lowest lying potential associated with the lowest total electron spin. This is the potential responsible for the vibrational energy levels observed in the stable diatomic molecule. The distinctive feature of this potential is its negative well which is very deep compared with the kinetic energy of collisions at the temperatures of interest herein. In fact, the depth of this well is just the dissociation energy of the diatomic molecules. As pointed out previously this energy corresponds to temperatures of about $50{,}000^{\circ}$ K for oxygen and of about $100{,}000^{\circ}$ K for nitrogen. Consider the collisions illustrated by the paths of the three black balls rolling into this potential well (fig. 11). The atom, which has a kinetic energy much larger than the absolute value of the potential field through which it traverses, will not be greatly deflected. Now it is the absolute value of the deflection produced by a collision which influences the flux of mass, momentum, or energy through the gas; hence, for practical purposes this collision, which produced only a small deflection, may be considered a miss. On the other hand, an atom which penetrates the volume where the potential change is about equal to its kinetic energy will suffer a considerable deflection, and such a collision will count. It is not essential that the repulsive, positive portion of the potential be penetrated, as in the third collision shown on the right in figure 11. In the subsequent estimates of the transport properties, it will be assumed that the effective diameter for atom-atom collisions is where the lowest lying potential equals $-kT$ and that the diameter for atom-molecule collisions is the arithmetic average of the atom-atom and the molecule-molecule diameters. This latter assumption corresponds to the concept that the collision diameter is a measure of the effective range of the electron distribution about the nucleus and that a collision occurs whenever these electron distributions overlap. In the case of collisions between ions or between electrons, the well-known coulomb potential $\pm e^2/r$ may be used in a similar way. For collisions between a neutral and a charged particle, the potential for the interaction between the charge and the induced dipole is used.

The coefficient of viscosity, which is based on the preceding assumption (ref. 5), is shown in figure 12 as a function of temperature for three pressures: 1.0, 0.01, and 0.0001 atmosphere. The ordinate is the ratio of the viscosity coefficient to the value given by a Sutherland type formula

$$\mu_o = 1.46 \times 10^{-5} T^{1/2} \left(1 + \frac{112}{T}\right)^{-1} \tag{10}$$

(in units of g/cm-sec). The ratio is unity until dissociation of molecules becomes appreciable; then the mean free path between molecular collisions becomes larger because the collision diameters for the atoms are smaller than for the molecules, the momentum exchange takes place between more widely separated planes in the gas, and the viscosity increases. On the other hand, the collision diameters become very large in an ionized gas, and then the reverse effect causes the viscosity to drop to very low values. Again, because of the regularity of the functions, it is possible to establish an empirical formula which approximates the temperature and pressure effect on viscosity. Such a formula is

$$\frac{\mu}{\mu_o} = \left\{1 + 0.023 \frac{T}{1000}\left[1 + \tanh \frac{\frac{T}{1000}\left(1 - \frac{1}{8} \log \frac{p}{p_o}\right) - 6.5}{1.5 + \frac{1}{8} \log \frac{p}{p_o}}\right]\right\} \times \exp^{-1}\left(\frac{\frac{T}{1000} - 14.5 - 1.5 \log \frac{p}{p_o}}{0.9 + 0.1 \log \frac{p}{p_o}}\right) \tag{11}$$

(log signifies the logarithm to the base 10). The comparison between equation (11) and the viscosity function is shown in figure 12.

The coefficient of thermal conductivity is shown as a function of temperature for pressures of 1.0 and 0.01 atmosphere in figure 13. Again, the coefficient is referenced to a coefficient of the Sutherland form:

$$k_o = 4.76 \times 10^{-6} T^{1/2} \left(1 + \frac{112}{T}\right)^{-1} \tag{12}$$

(in units of cal/cm-sec-$^\circ$K). The calculation of these coefficients is based on the method outlined by Hirschfelder (ref. 11) and developed further by Butler and Brokaw (ref. 12). In this method, the energy transfer through the gas is treated in two independent parts. One part is the energy transferred by collisions as in ordinary thermal conductivity of nonreacting gases. The other part is the energy transferred by diffusion of the gas particles and the reactions which occur to reestablish chemical equilibrium. This latter part predominates wherever the compressibility derivative with respect to temperature becomes a maximum. The effect is very much like the effect on the specific heats. In fact, the thermal conductivity ratio k/k_o is nearly proportional to the specific heat just as for inert gases, so that a reasonably good approximation is

$$\frac{k}{k_o} \approx \frac{c_p}{3.5R} \tag{13a}$$

The comparison between the thermal conductivity and the approximate specific heat given by equation (8) is indicated in figure 13. Note that the symbol k is conventionally used for both Boltzmann's constant and thermal conductivity. Wherever kT appears, k signifies Boltzmann's constant.

The relation given by equation (13a) is good only for the dissociation reactions. Where ionization occurs, the thermal conductivity is greatly increased because of the high thermal velocity of the lightweight electrons. Then the thermal conductivity is approximately given up to about 10 percent ionization by

$$\frac{k}{k_o} \approx 3\left(1 + \frac{1}{4} \log \frac{p}{p_o}\right)\frac{c_p}{3.5R} \tag{13b}$$

It is desirable to check the foregoing theoretical calculations and approximations with experiment. One of the more striking effects predicted by the theory is the pronounced effect on thermal conductivity of gases in which chemical reactions occur. This effect has been observed experimentally in dissociating N_2O_4 by Coffin and O'Neal at the Lewis Flight Propulsion Laboratory (ref. 13). As figure 14 shows, their experiments are in very good agreement with the theoretical prediction for the equilibrium gas. The results strongly suggest that the basic relations established by Hirschfelder (ref. 11) are essentially correct. Unfortunately, the thermal dissociation of air cannot be studied at such tractable temperatures as in the case of N_2O_4. However, high-temperature air can be produced in the shock tube for short intervals, and figure 15 shows the correlation between measured and theoretical thermal conductivity in air, which has been obtained at the Ames Aeronautical Laboratory. In these experiments, strong shock waves are reflected from the closed end of a shock tube, and a temperature is measured at the interface between the hot stationary air and a quartz glass plug. The temperature is deduced by measuring the change in resistance of a thin film of nickel evaporated onto the glass. If it is assumed that the air is in equilibrium and has a constant thermal diffusivity $k/c_p\rho$, the interface temperature rises instantaneously to a constant value which is related to the diffusivity of air and of the glass plug (ref. 14). As will be pointed out later, the dissociation of air may be rapid enough to justify the assumption of instantaneous equilibrium. Thermal diffusivity will not be constant in the air, of course, but at least the strong variations in heat capacity and thermal conductivity will cancel each other. In any event, when the experimental data are correlated in this manner, they compare reasonably well with the theoretical predictions. No consistent data exist yet in the really interesting region where a maximum in the coefficient is predicted because of oxygen dissociation.

To illustrate the manner in which the transport properties enter some aerodynamic calculations, consider the heat transfer to the stagnation region of a blunt, high-speed vehicle with a cool wall. According to reference 15, an approximate expression for this heat transfer is

$$\frac{qr}{\sqrt{Re}} = \left(\frac{\rho_2}{\rho_1} - 1\right)^{1/4}\left(\frac{\mu_1}{\mu_2}\right)^{1/2}\int_0^{T_2} k\, dT \qquad (14)$$

where q is the heat flux per unit area at the stagnation point, r is the radius of curvature of the vehicle at this point, and Re is the Reynolds number based on the length r and free-stream conditions. These free-stream conditions are designated by the subscript 1 and, as before, the subscript 2 refers to conditions following the shock wave. At moderate altitudes, below 150,000 feet for example, the air in the stagnation region is essentially everywhere in equilibrium, as will be pointed out later. Thus the equilibrium thermodynamic properties of air may be used to evaluate the density ρ_2 and the temperature T_2. The viscosity μ_2 and the thermal conductivity k for air in equilibrium are functions of temperature uniquely determined by the pressure p_2, and they are given approximately by equations (11) and (13a), respectively. Thus the evaluation of the heat-transfer parameter, given by equation (14), is relatively straightforward and this parameter is given as a function of velocity in figure 16. The effect of the changes in ambient conditions with altitude is rather small and has not been shown. Figure 16 also shows that there is satisfactory agreement between the theoretical solution and the experimental results reported by Rose and Riddell (ref. 16). This solution also agrees with the fairly rigorous deductions of stagnation-point heat transfer developed by Fay and Riddell (ref. 17). The approximate expression (eq. (14)) is useful here because the role of the transport properties is easy to visualize in view of the simple form of the functional relationships involved.

When one considers the flow processes which occur in high-speed flight at very high altitudes, or in regions of highly expanded flow, the equilibrium thermodynamic and transport properties may not be sufficient to determine the flow uniquely. At the very low densities which occur in these cases, the time required for the approach to equilibrium may be comparable to the time needed for a sample of air to pass through a disturbed region of the flow field. Then the chemical reaction rates become another set of independent parameters on which the flow depends. These are discussed in the following section.

CHEMICAL REACTION RATES

Before discussing the finite reaction rates, simple flows are compared for the two limiting cases: (1) The reaction is frozen and (2) the reaction is in equilibrium.

The effects of chemical reactions on the equilibrium conditions following a normal shock may be seen from figure 8. In order to compare three of the state variables simultaneously, the density, pressure, and temperature effects are shown together in figure 17 for flight at 160,000 feet altitude. If the reactions were infinitely slow, air would behave as an ideal gas. This condition is designated as frozen flow, and it corresponds to the reference value of unity in figure 17. However, the reaction rates are finite and, as the flow approaches equilibrium, the temperature is greatly reduced because thermal energy is soaked up in exciting vibrations and in breaking chemical bonds. The pressure is not greatly influenced by the reactions, and the drop in temperature is compensated by a large increase in density.

Reference 18 gives an analysis for flow that maintains chemical equilibrium while expanding around a corner, and a numerical example is given in figure 18 for air which is initially at 6,140° K and 1.2 atmospheres. The effect of the reaction in this case is to increase the temperature over the nonreacting value because the recombining gas now gives up the energy that is contained in dissociation and vibration. Thus the gas cools much more slowly during the expansion than a nonreacting gas. From figure 18 it is seen that, during the Prandtl-Meyer expansion, it is the density which is relatively little affected by the reactions and that it is the pressure which adjusts with the temperature change this time. This is in marked constrast to the effects of reactions on the shock compression.

Now the reaction rates depend on the number of molecular collisions per unit time, and these collisions are more frequent the higher the density and the higher the temperature. At the high densities which occur in low altitude flight, the rates are very rapid and air flows are essentially in complete equilibrium. On the other hand, at very high altitudes where densities are very low, the reaction rates are so slow that flow may be essentially frozen. At intermediate altitudes, it is necessary to consider the reaction rate, from which can be derived the characteristic time in which the gas decays to chemical equilibrium. In a flowing gas, the quantity of interest is a characteristic length obtained by multiplying the time by the flow speed. This characteristic length is used for example in calculations of one-dimensional flows in references 19 and 20.

Figure 19 shows the lengths required to reach vibrational equilibrium in the flow downstream of a normal shock wave at various altitudes and velocities. Relaxation effects are important where this length compares in magnitude with a length such as the shock-detachment distance. At low velocities, where low temperatures occur, the reactions have a trivial effect, as indicated by the shaded portion of the figure. It is seen that, for a wide range of speeds and altitudes, the vibrations may be regarded as being in equilibrium. At altitudes below 150,000 feet, the finite length generally needs to be considered only for vehicles

moving slower than 10,000 feet per second. At 240,000 feet, the vibrational relaxation will be important at the stagnation region for vehicles traveling less than 25,000 feet per second. The calculations for these curves are based on Blackman's experimental values for vibrational relaxation (ref. 21). These agree fairly well with the theory of Schwartz and Herzfeld (ref. 22) and the calculations are probably correct within a factor of 5, at least. In contrast, the existing knowledge of dissociation rates is extremely uncertain. The theoretical calculations require some severe mathematical approximations (ref. 23), and experiments have been made only recently which fix the reaction rates within several orders of magnitude (refs. 24, 25, and 26). Despite the value of these recent data, the state of knowledge is still far from satisfactory, as is illustrated in figure 20. This figure shows the three-body recombination rate as a function of temperature for the recombination of oxygen and nitrogen atoms and for the recombination of atoms in air. The third body M in the collision serves to carry away the excess energy released by the recombination so that the newly formed molecule can be stable. The fact that the results do not agree more closely is only partly due to experimental uncertainties, since there also exists some question of how to translate the observed relaxation times into reaction rates. In view of these uncertainties, the theory developed by Wigner (ref. 23) has been used to calculate the characteristic reaction lengths in dissociating flow. In applying this theory it has been assumed that the third body in the recombination reaction is a hard elastic sphere and that the potential between atoms is the same one used earlier to evaluate the transport properties. The same expression is used for the recombination rate of both the oxygen and nitrogen atoms.

Figure 21 shows the results for the flow lengths required to reach oxygen dissociation equilibrium downstream of a normal shock. The same functional relations occur as for vibrations; that is, relaxation becomes increasingly important at higher altitudes and lower velocities. For nitrogen dissociation, all curves in figure 16 would be shifted to the left so that the curve for a velocity of 10,000 feet per second for nitrogen roughly coincides with the curve for a velocity of 15,000 feet per second for oxygen; it would fall in the "reaction negligible" region. (See fig. 1.) Similarly, the curve of 15,000 feet per second for nitrogen shifts roughly to the curve of 20,000 feet per second for oxygen.

Above an alitutde of 250,000 feet, the typical vehicle enters slip flow and, as the altitude increases further, the shock wave eventually disappears. Under these conditions, molecular impact on surfaces is a more important phenomenon than those associated with the continuum airflow properties. Thus, in any case, the relaxation effects need to be considered only over a finite range of velocity and altitude.

CONCLUDING REMARKS

It has been found that a fairly satisfactory state of scientific knowledge exists with respect to the equilibrium thermodynamic properties of air, that the knowledge of the transport properties leaves something to be desired, and that the state of theory and experiment on chemical reaction rates is quite inadequate. For example, equilibrium thermodynamic properties can be calculated very precisely by iteration methods, to the order of 1/2 percent or better; closed-form analytic solutions for these properties are accurate to the order of 2 to 5 percent; and approximate semiempirical formulas are available for rough engineering estimates which are good to the order of 10 to 20 percent. For transport properties, good theoretical methods for calculating collision cross sections are not yet available; the approximations used have an uncertainty of the order of 50 percent, but the order of magnitude and the functional relationships which have been estimated for these properties are probably correct. Vibrational relaxation rates are approximately known, but the dissociation rates are still uncertain by several orders of magnitude. However, much effort is being focused on these problems, and it is reasonable to anticipate that adequate solutions for aerodynamic purposes will soon be forthcoming.

Ames Aeronautical Laboratory
National Advisory Committee for Aeronautics
Moffett Field, Calif., Mar. 19, 1958

REFERENCES

1. Herzberg, Gerhard: Molecular Spectra and Molecular Structure. I. Spectra of Diatomic Molecules. Second ed., D. Van Nostrand Co., Inc., 1950-51.

2. Moore, Charlotte E.: Atomic Energy Levels. Cir. 467, Nat. Bur. Standards, vol. I, sect. I, April 15, 1948.

3. Gilmore, F. R.: Equilibrium Composition and Thermodynamic Properties of Air to 24,000° K. RAND Res. Memo. RM-1543, The RAND Corp., Aug. 24, 1955. (Also available from ASTIA as AD 84052.)

4. Hilsenrath, Joseph, and Beckett, Charles W.: Tables of Thermodynamic Properties of Argon-Free Air to 15,000° K. AEDC-TN-56-12, Arnold Eng. Dev. Center, Sept. 1956. (Also available from ASTIA as Doc. No. AD-98974.)

5. Hansen, C. Frederick: Approximations for the Thermodynamic and Transport Properties of High-Temperature Air. NACA TN 4150, 1958.

6. Feldman, Saul: Hypersonic Gas Dynamic Charts for Equilibrium Air. AVCO Res. Lab., Jan. 1957.

7. Romig, Mary F.: The Normal Shock Properties for Air in Dissociation Equilibrium. Jour. Aero. Sci., vol. 23, no. 2, Feb. 1956, p. 185.

8. Hochstim, Adolf R.: Gas Properties Behind Shocks at Hypersonic Velocities. I. Normal Shocks in Air. Rep. No. ZPh(GP)-002, CONVAIR, Jan. 30, 1957.

9. Hirschfelder, Joseph O., Curtiss, Charles F., and Bird, R. Byron: Molecular Theory of Gases and Liquids. John Wiley & Sons, Inc., 1954.

10. Kennard, Earle H.: Kinetic Theory of Gases. McGraw-Hill Book Co., Inc., 1938.

11. Hirschfelder, Joseph O.: Heat Transfer in Chemically Reacting Gas Mixtures. Jour. Chem. Phys., vol. 26, no. 2, Feb. 1957, pp. 274-281.

12. Butler, James N., and Brokaw, Richard S.: Thermal Conductivity of Gas Mixtures in Chemical Equilibrium. Jour. Chem. Phys., vol. 26, no. 6, June 1957, pp. 1636-1643.

13. Coffin, Kenneth P., and O'Neal, Cleveland, Jr.: Experimental Thermal Conductivities of the $N_2O_4 \rightleftarrows 2NO_2$ System. NACA TN 4209, 1958.

14. Mersman, W. A., Berggren, W. P., and Boelter, L. M. K.: The Conduction of Heat in Composite Infinite Solids. Univ. of California Pub. in Eng., vol. 5, no. 1, 1942, pp. 1-22.

15. Eggers, A. J., Jr., Hansen, C. Frederick, and Cunningham, Bernard E.: Stagnation-Point Heat Transfer to Blunt Shapes in Hypersonic Flight, Including Effects of Yaw. NACA TN 4229, 1958. (Supersedes NACA RM A55E02)

16. Rose, Peter H., and Riddell, F. R.: An Investigation of Stagnation Point Heat Transfer in Dissociated Air. AVCO Res. Lab. Rep. No. 7, April 1957.

17. Fay, J. A., and Riddell, F. R.: Theory of Stagnation Point Heat Transfer in Dissociated Air. AVCO Res. Lab. Rep. No. 1, June 1956 (Rev. April 1957).

18. Heims, Steve P.: Prandtl-Meyer Expansion of Chemically Reacting Gases in Local Chemical and Thermodynamic Equilibrium. NACA TN 4230, 1958.

19. Talbot, L.: The Structure of a Shock Wave in a Gas Having a Long Relaxation Time. Tech. Rep. HE-150-145, Inst. Eng. Res., Univ. of California, Mar. 1957.

20. Heims, Steve P.: Effect of Oxygen Recombination on One-Dimensional Flow at High Mach Numbers. NACA TN 4144, 1958.

21. Blackman, V.: Vibrational Relaxation in Oxygen and Nitrogen. Jour. Fluid Mech., vol. 1, pt. 1, May 1956, pp. 61-85.

22. Schwartz, Robert N., and Herzfeld, Karl F.: Vibrational Relaxation in Gases (Three Dimensional Treatment). Jour. Chem. Phys., vol. 22, no. 5, May 1954, pp. 767-776.

23. Wigner, E.: Calculation of the Rate of Elementary Association Reactions. Jour. Chem. Phys., vol. 5, no. 9, Sept. 1937, pp. 720-725.

24. Camac, M., Camm, J., Feldman, S., Keck, J., and Petty, C.: Chemical Relaxation in Air, Oxygen and Nitrogen. IAS Preprint No. 802, Jan. 1958.

25. Christian, R. H., Duff, R. E., and Yarger, F. L.: Equation of State of Gases by Shock Wave Measurements. II. The Dissociation Energy of Nitrogen. Jour. Chem. Phys., vol. 23, no. 11, Nov. 1955, pp. 2045-2049.

26. Logan, Joseph G., Jr.: Relaxation Phenomena in Hypersonic Aerodynamics. IAS Preprint No. 728, Jan. 1957.

STAGNATION REGION CHEMISTRY

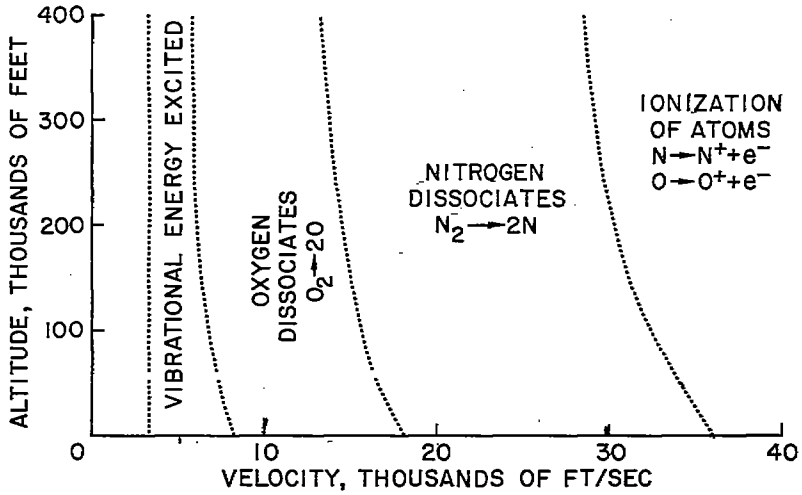

Figure 1

DIATOMIC MOLECULE

ENERGY

$$e(u,J,n) = \frac{mu^2}{2} + J(J+1)\frac{h^2}{2I} + nh\nu$$

AVERAGE ENERGY

$$E = \frac{3}{2}RT + RT + RT\left(\frac{h\nu}{kT}\right)\left(e^{\frac{h\nu}{kT}} - 1\right)^{-1}$$

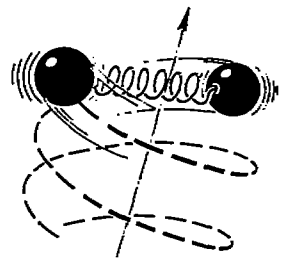

SPECIFIC HEAT, $\frac{dE}{dT}$

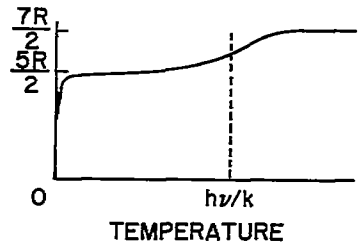

Figure 2(a)

ATOMS

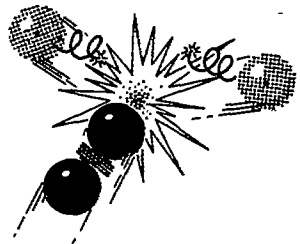

ENERGY

$$e(u)=\left(\frac{m}{2}\right)\frac{u^2}{2}+\frac{e_0}{2}$$

AVERAGE ENERGY

$$E=\frac{3}{2}RT+\frac{D}{2}$$

SPECIFIC HEAT

$$\frac{dE}{dT}=\frac{3}{2}R$$

Figure 2(b)

MOLECULE-ATOM MIXTURES IN EQUILIBRIUM

ENERGY:

$$E=(1-x)E_m+xE_a$$

SPECIFIC HEAT:

$$\frac{\partial E}{\partial T}=(1-x)\frac{dE_m}{dT}+x\frac{dE_a}{dT}$$
$$-E_m\frac{\partial x}{\partial T}+(E_a)\frac{\partial x}{\partial T}$$

mol fraction:

$$x=f(K,p)$$

mol fraction derivative:

$$\frac{\partial x}{\partial T}=g\left(\frac{\partial \log_e K}{\partial T},\ x\right)$$

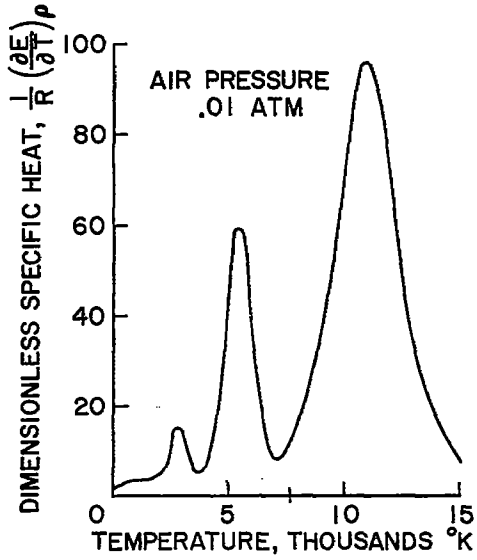

Figure 3

COMPRESSIBILITY FOR AIR IN EQUILIBRIUM

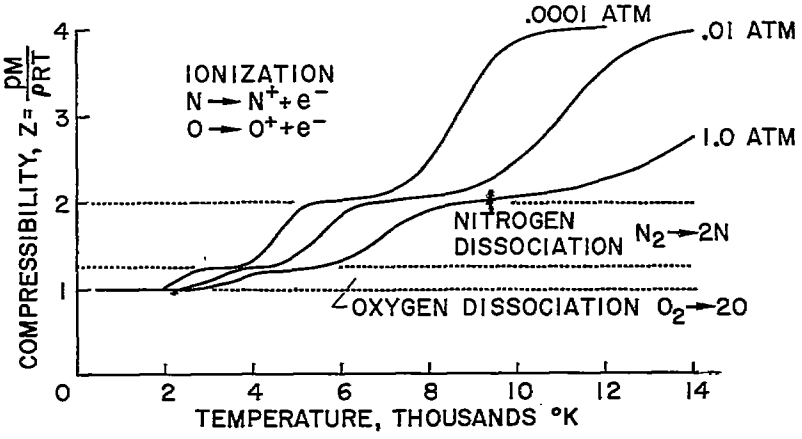

Figure 4

ENERGY OF AIR IN EQUILIBRIUM

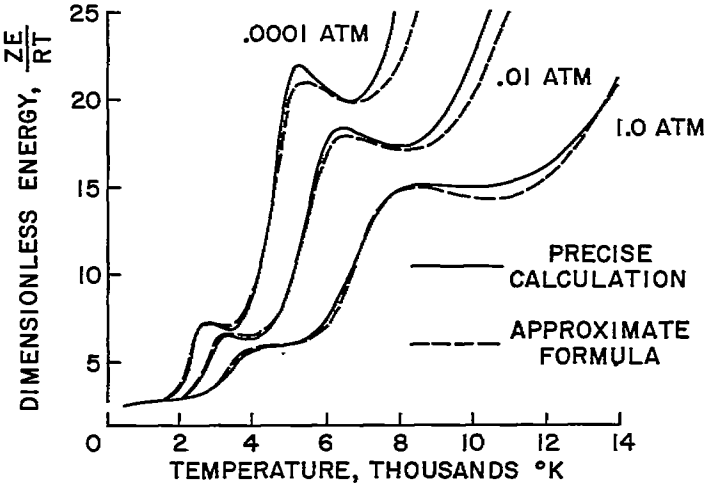

Figure 5

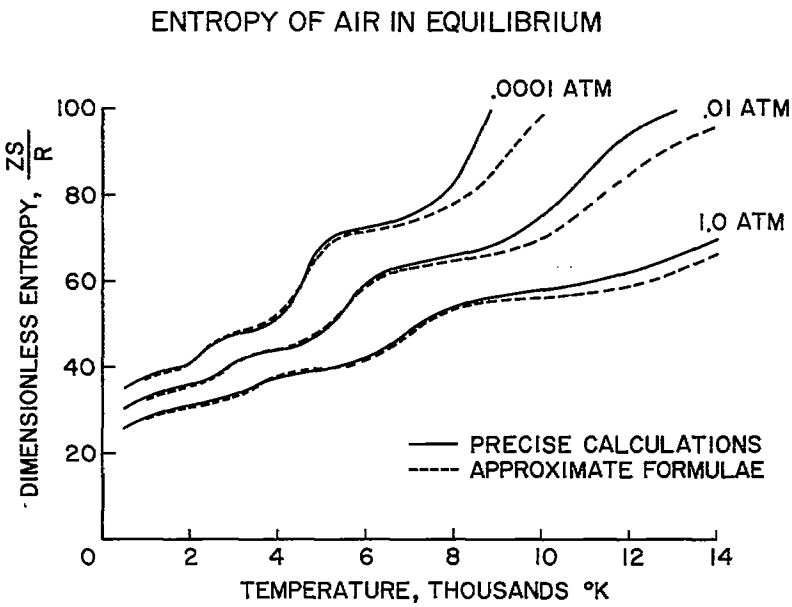

Figure 6

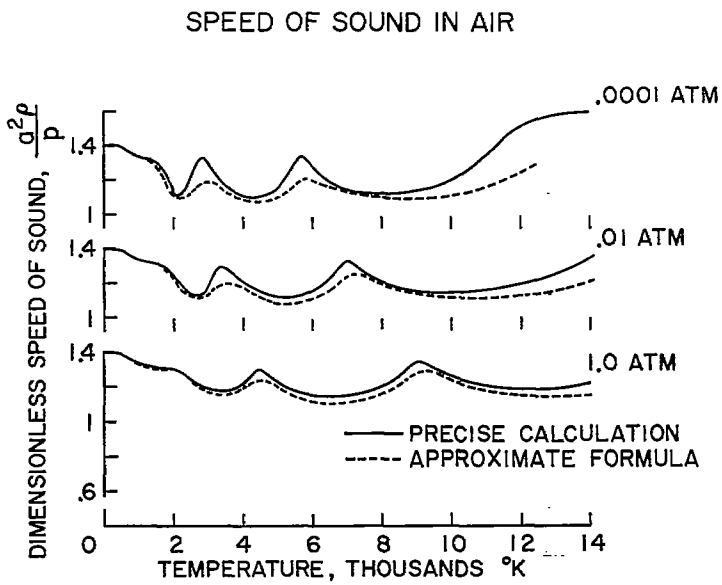

Figure 7

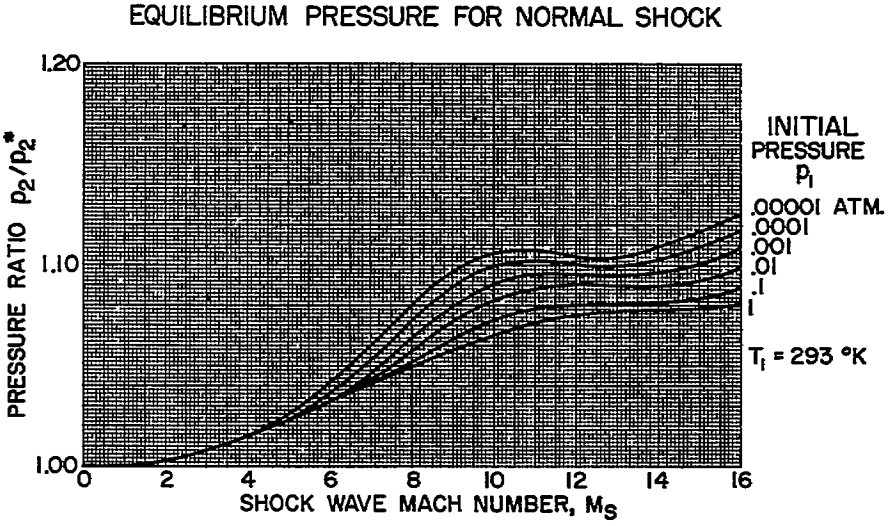

Figure 8(a)

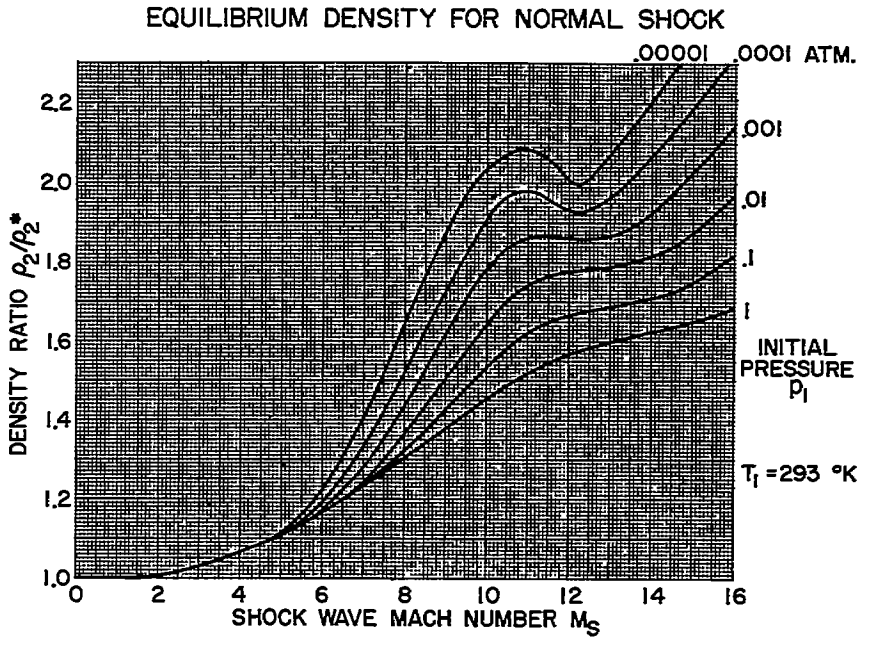

Figure 8(b)

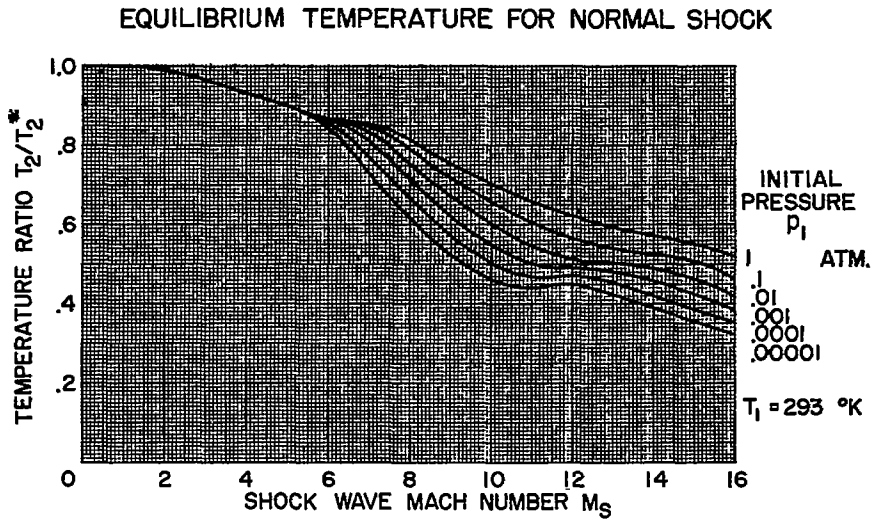

Figure 8(c)

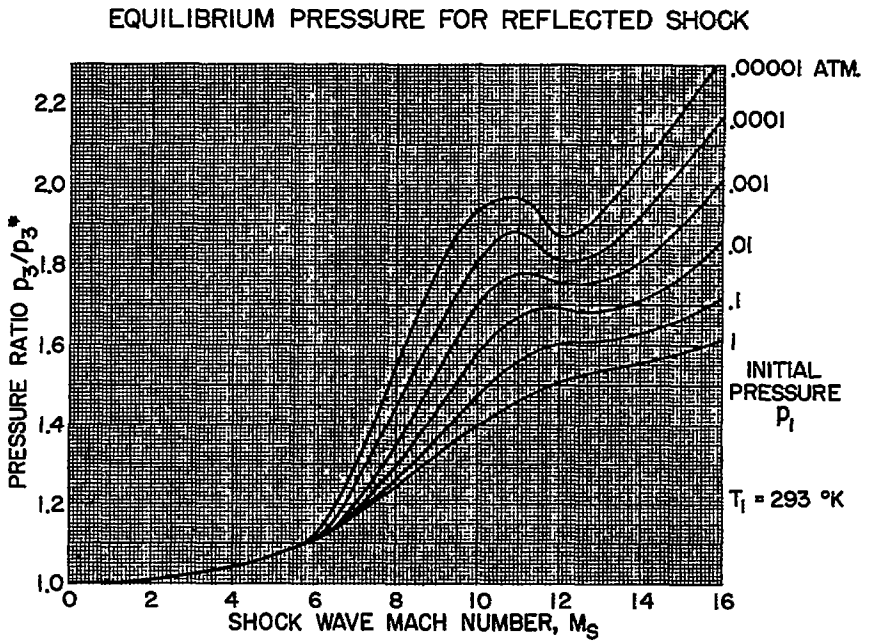

Figure 9(a)

EQUILIBRIUM DENSITY FOR REFLECTED SHOCK

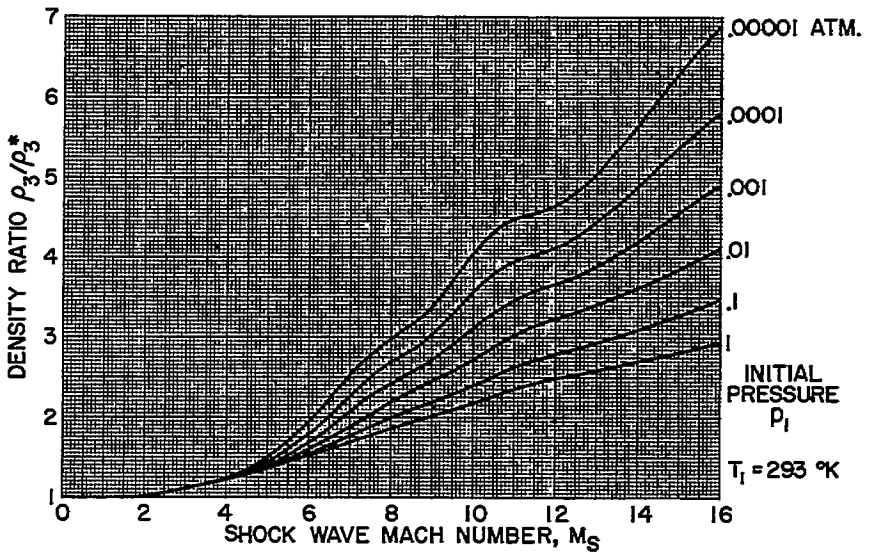

Figure 9(b)

EQUILIBRIUM TEMPERATURE FOR REFLECTED SHOCK

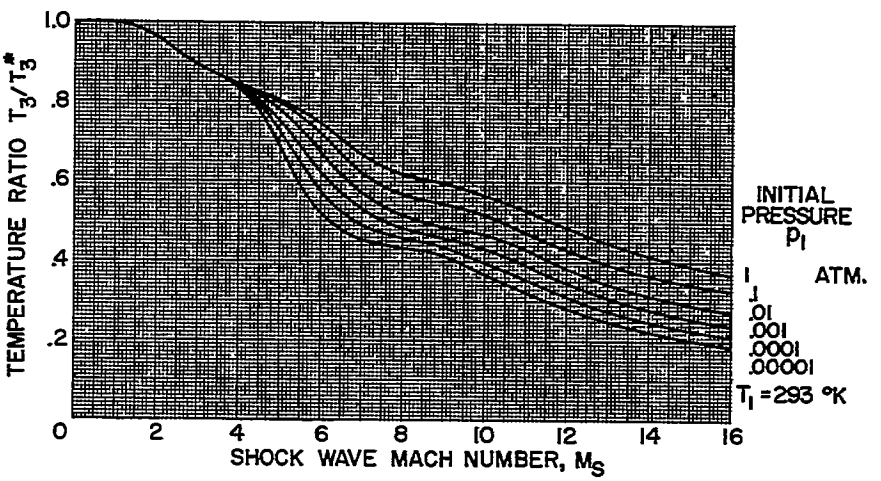

Figure 9(c)

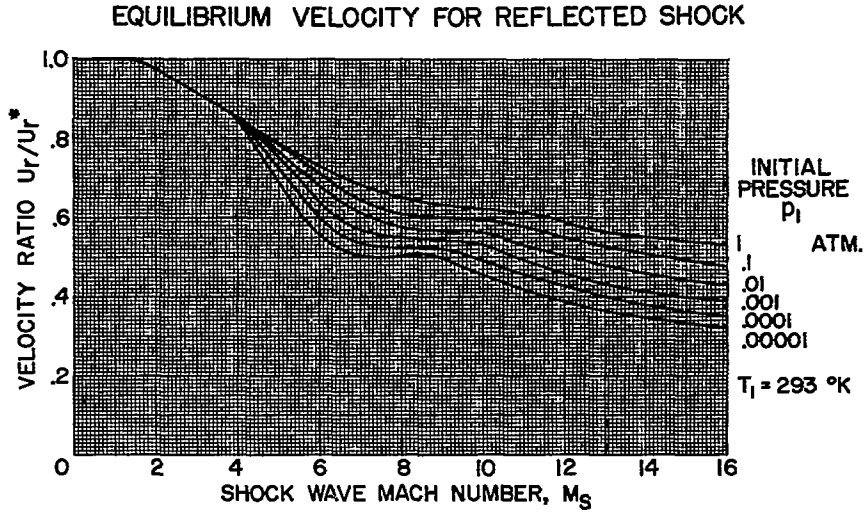

Figure 10

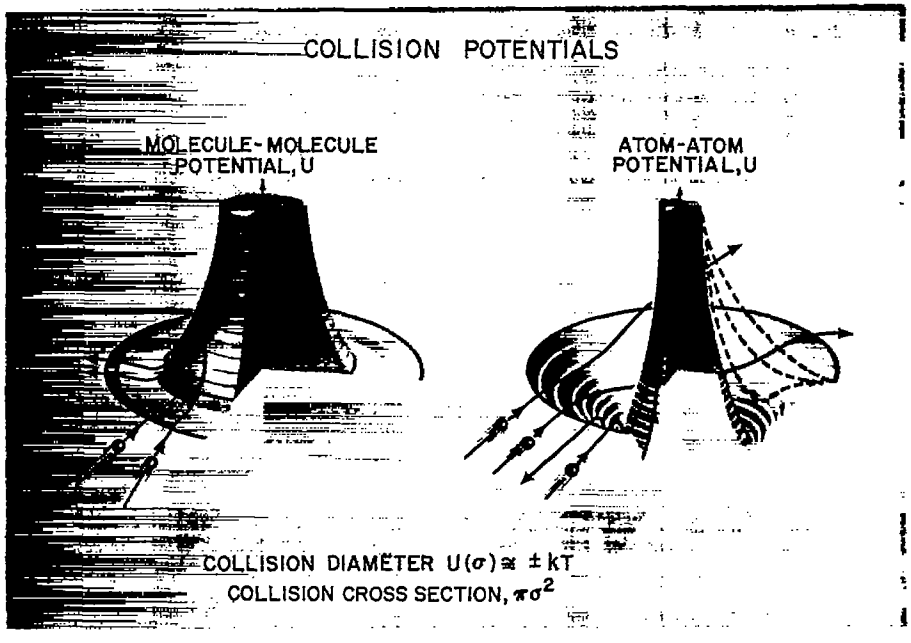

Figure 11

VISCOSITY FOR AIR

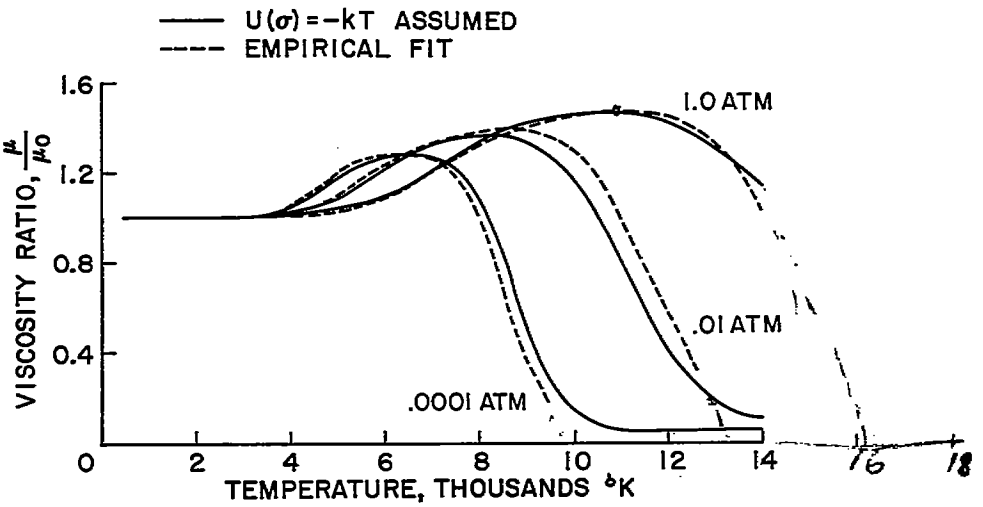

Figure 12

THERMAL CONDUCTIVITY FOR AIR

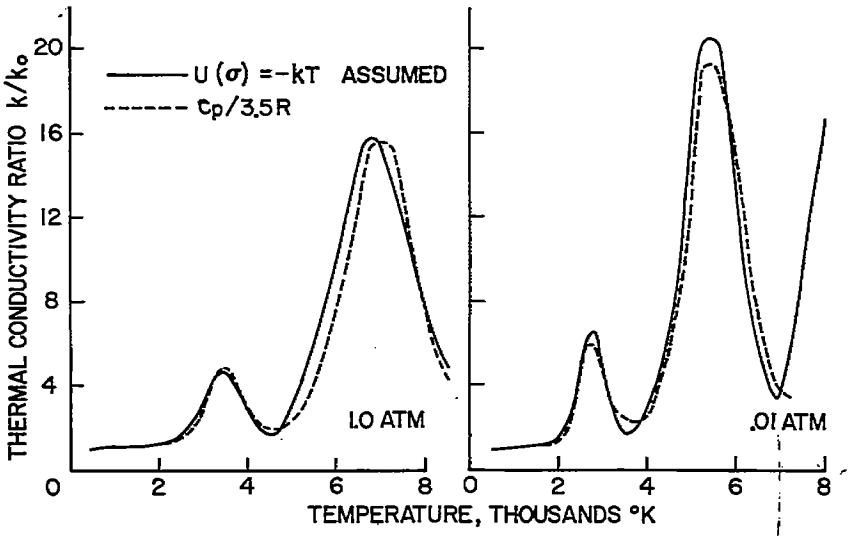

Figure 13

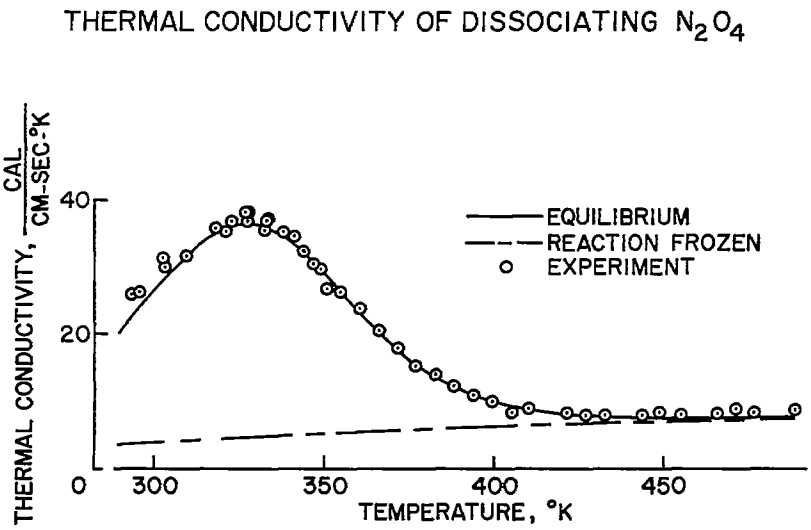

Figure 14

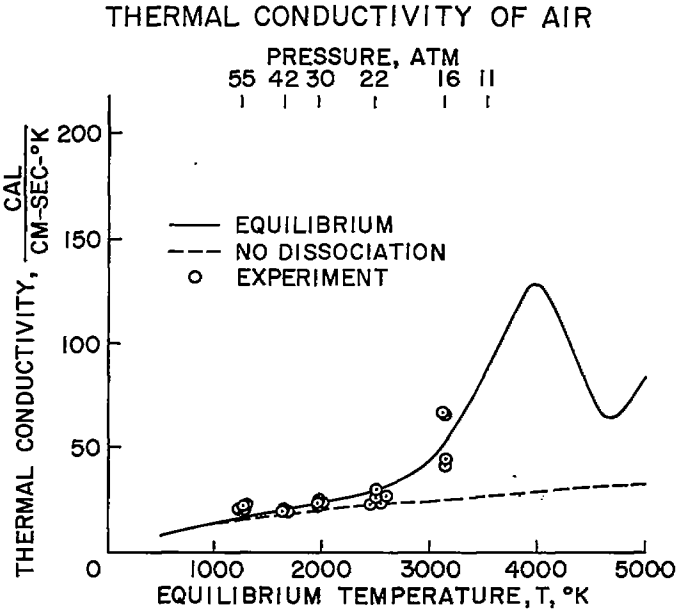

Figure 15

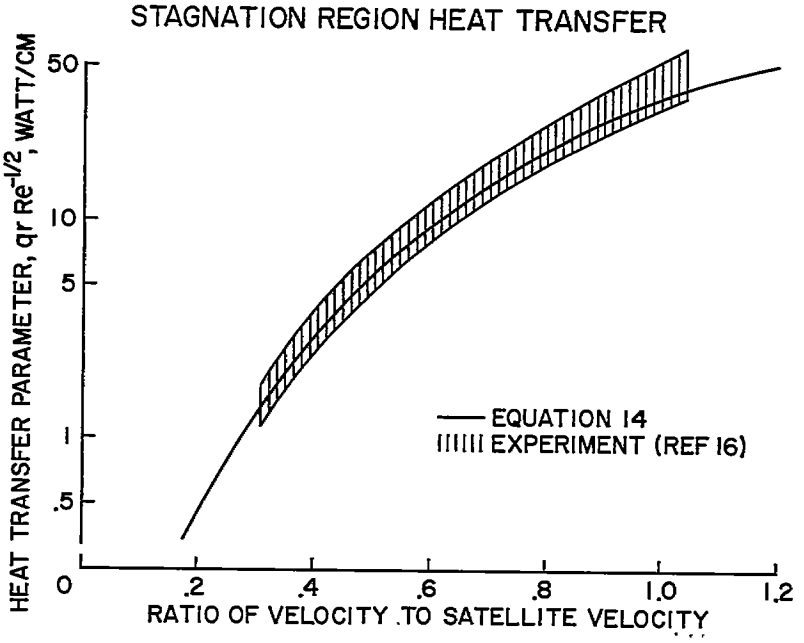

Figure 16

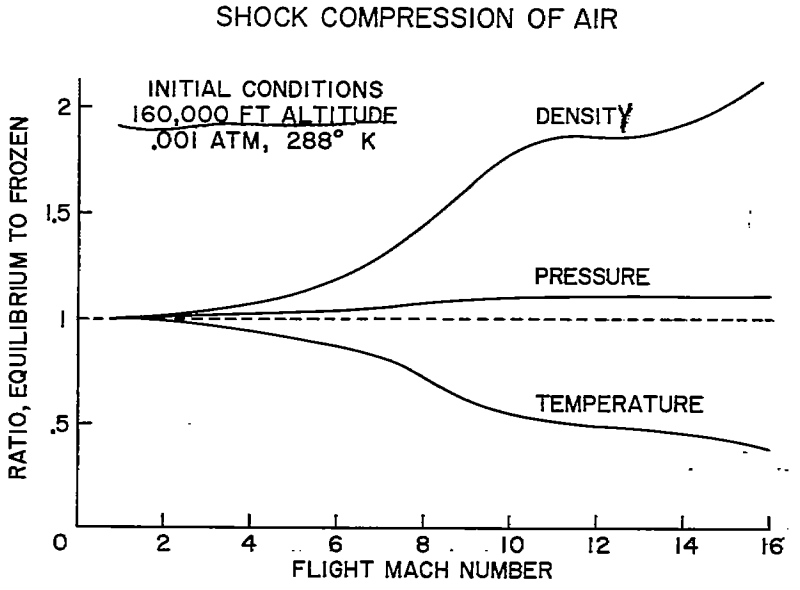

Figure 17

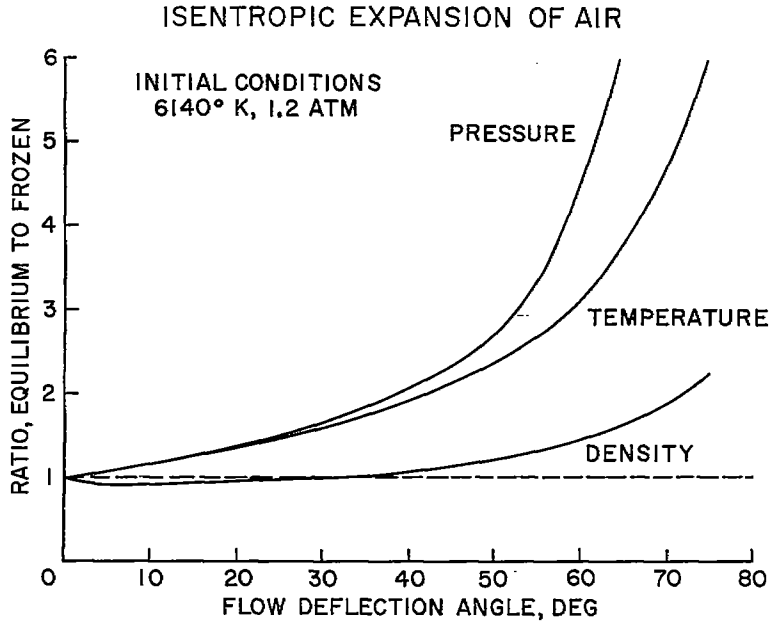

Figure 18

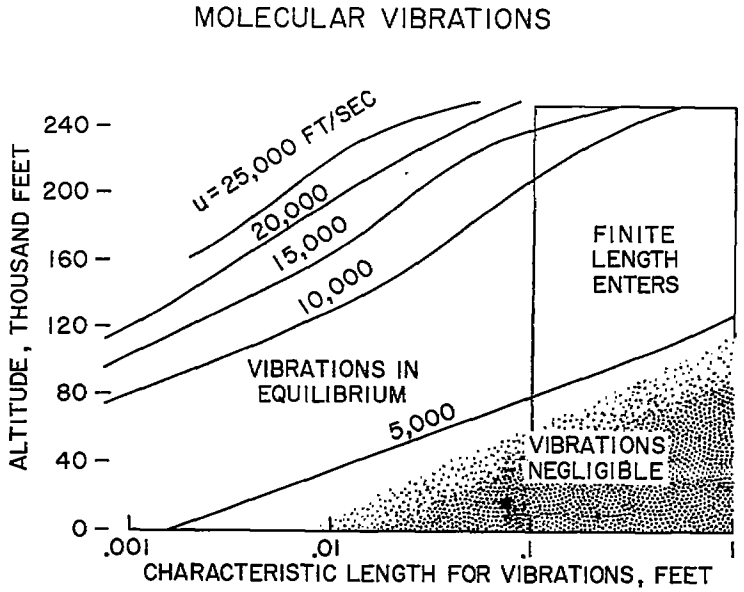

Figure 19

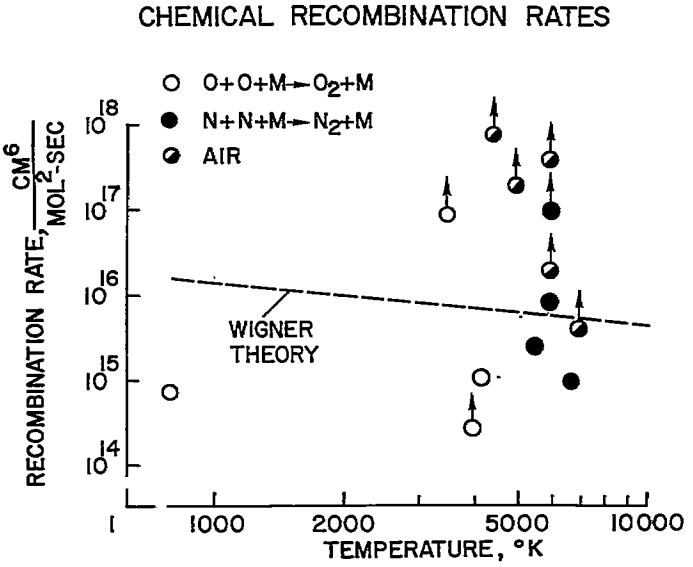

Figure 20

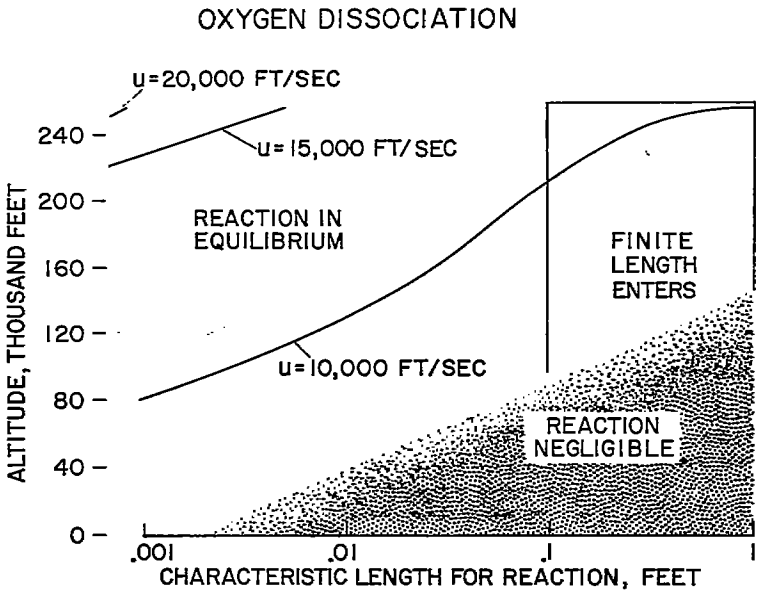

Figure 21